PAPER

NJC
www.rsc.org/njc

^{1}H NMR analysis of porphyrin-stoppered rotaxanes: effect of the porphyrin substituents on the macrocycle†

Taichi Ikeda, Masumi Asakawa and Toshimi Shimizu*

Nanoarchitectonics Research Center, National Institute of Advanced Industrial Science and Technology (AIST), Tsukuba Central 5, 1-1-1 Higashi, Tsukuba, Ibaraki 305-8565, Japan
E-mail: tshmz-shimizu@aist.go.jp; Fax: +81 298 61 4545; Tel: +81 298 61 4544

Received* (in Durham, UK) *10th March 2004, Accepted 28th April 2004
First published as an Advance Article on the web 15th June 2004

Six kinds of porphyrin-stoppered rotaxanes were prepared by the combination of two threads (relatively longer and shorter) and three porphyrin rhodium chlorides having different substituents. The chemical shift changes in ^{1}H NMR spectra, due to the anisotropic shielding effects by the aromatic rings, enabled us to estimate the molecular structure. In the cases of the rotaxanes with relatively shorter thread, the conformation of the macrocycle proved to be affected by the substituents in the terminal porphyrin. This result suggests a mechanical interaction between the macrocycle and terminal porphyrin. This result will lead to novel designing of the molecular devices that can regulate the rotational motion of the macrocycle by the terminal porphyrin or transmit the rotational motion from the macrocycle to the terminal porphyrin.

Introduction

Interlocked molecules such as the rotaxanes and catenanes have attracted increasing attention as new functional materials having mechanical motion (translational or rotational motion) between the components.[1–4] The mechanical motions are applicable to the molecular shuttles,[1] molecular switches,[2] molecular motors[3] and molecular muscles.[4] Recently, it has been possible to prepare interlocked molecules through thermodynamically stable noncovalent bonds.[5–7] Using this approach, one can easily obtain interlocked molecules in high yields. We have reported porphyrin-stoppered rotaxanes using the axial coordination bond of porphyrin rhodium(III) chloride and the host–guest system between the secondary ammonium cation group and dibenzo-24-crown-8 (DB24C8).[5,6] In the case of 5,10,15,20-tetraphenylporphyrin (TPP) stoppered rotaxane, we were able to analyze the molecular structure using X-ray crystallography.[6] As for other rotaxanes capped with 2,3,7,8,12,13,17,18-octaethylporphyrin (OEP) and 5,10,15,20-tetra[3,5-di(*tert*-butyl)phenyl]porphyrin (TBPP) rhodium chlorides, no single crystal was obtainable. Therefore, we had no direct information on the molecular structure of these porphyrin-stoppered rotaxanes using X-ray crystallography. However, the chemical shift changes in ^{1}H NMR spectra, due to the anisotropic shielding effect by the porphyrin[6,8] and the catechol rings of DB24C8, enabled us to estimate the molecular structure. In this study, we analyzed six kinds of porphyrin-stoppered rotaxanes using ^{1}H NMR. On the basis of this analysis, we discuss the effect of the porphyrin substituents on the conformation of the macrocycle in the rotaxane.

Experimental

General

OEP and TPP were purchased from Tokyo Chemical Industry Co. TBPP was synthesized according to the literature.[9] The preparations of porphyrin rhodium chlorides,[6,8] two threads [relatively long (L) and short (S)][5,6] and porphyrin-stoppered rotaxane[5,6] are described in the references. All chemical reagents and solvents were commercially available and used as received. ^{1}H and ^{13}C NMR spectra were recorded on a Bruker AVANCE 400 spectrometer (400 and 100 MHz for ^{1}H and ^{13}C NMR, respectively) with use of residual solvent as the internal standard. ^{1}H NMR and ^{13}C NMR spectra were assigned using 2D COSY, ROESY, HMQC and HMBC. All NMR measurements were conducted at 293 K.

Product characterization data

Rotaxane Rx(OEP · L). Orange solid (Yield: 80%). ^{1}H NMR (400 MHz, $CDCl_3$): δ 0.12 (d, $J = 7.0$ Hz, 2H, $C^{11}H$), 1.19 (s, 3H, C^aH_3), 1.99 (t, 12H, CH_3), 3.07 (m, 8H, $C^\gamma H_2$), 3.45 (m, 8H, $C^\beta H_2$), 3.82 (m, 8H, $C^\alpha H_2$), 4.11 (q, 8H, CH_2), 4.21 (br, 2H, C^bH_2), 4.42 (br, 2H, C^cH_2), 5.50 (d, $J = 7.0$ Hz, 2H, $C^{10}H$), 6.52 (m, 4H, $C^{13}H$), 6.70 (m, 4H, $C^{12}H$), 6.92 (d, $J = 8.4$ Hz, 2H, C^3H), 7.04 (d, $J = 8.4$ Hz, 2H, C^6H), 7.06 (d, $J = 8.4$ Hz, 2H, C^2H), 7.37 (br, 2H, NH_2), 7.41 (d, $J = 8.4$ Hz, 2H, C^7H), 10.22 (s, 4H, $C_{meso}H$), 10.40 (s, 1H, CONH). ^{13}C NMR (100 MHz, $CDCl_3$): δ 19.0 (CH_3), 20.5 (CH_2), 31.6 (C^aH_3), 35.0 (C–C^aH_3), 52.3 (C^c), 52.6 (C^b), 68.5 (C^α), 70.3 (C^β), 70.7 (C^γ), 98.2 (*meso*), 112.6 (C^{10}), 113.1 (C^{13}), 122.2 (C^{12}), 125.8 (C^2), 128.7 (C^4), 128.8 (C^7), 129.1 (C^3, C^6), 135.0 (C^8), 135.2 (C^5), 140.1 (α-pyrrole), 142.8 (β-pyrrole), 145.3 (C^9), 146.2 (C^{11}), 147.6 (C^{14}), 152.8 (C^1), 166.5 (C=O). Anal. Calcd for $C_{86}H_{104}ClF_3N_7O_{11}Rh \cdot H_2O$: C 63.56, H 6.57, N 6.03; found: C 63.84, H 6.45, N 5.95%.

Rotaxane Rx(OEP·S). Orange solid (Yield: 75%). ^{1}H NMR (400 MHz, $CDCl_3$): δ 0.19 (d, $J = 6.8$ Hz, 2H, C^7H), 1.14 (s, 9H, C^aH_3), 1.92–2.02 (m, 12H, CH_3), 2.21 (m, 4H, $C^\gamma H_2$), 2.80 (overlapping, 8H, $C^\gamma H_2$ and $C^\beta H_2$), 3.20 (br, 2H, C^cH_2), 3.24 (overlapping, 8H, $C^\beta H_2$ and $C^\alpha H_2$), 3.60 (m, 4H, $C^\alpha H_2$), 3.74 (br, 2H, C^bH_2), 4.09–4.18 (m, 8H, CH_2), 4.80 (d, $J = 6.8$ Hz, 2H, C^6H), 6.22 (m, 4H, $C^{13}H$), 6.52 (br, 2H, NH_2), 6.68 (d, $J = 8.4$ Hz, 2H, C^3H), 6.71 (m, 4H, $C^{12}H$), 6.96 (d, $J = 8.4$ Hz, 2H, C^2H), 10.26 (s, 4H, $C_{meso}H$). ^{13}C NMR (100 MHz, $CDCl_3$): δ 19.2 (CH_3), 20.5 (CH_2), 31.5

† Electronic supplementary information (ESI) available: chemical shift data. See http://www.rsc.org/suppdata/nj/b4/b403707c/

DOI: 10.1039/b403707c

(C^a), 35.0 (C–C^aH_3), 48.8 (C^c), 51.9 (C^b), 68.2 (C^α), 69.8 (C^β), 70.2 (C^γ), 98.3 (*meso*), 112.9 (C^{13}), 122.2 (C^{12}), 122.5 (C^6), 125.7 (C^2), 128.2 (C^4), 129.1 (C^3), 140.0 (C^5), 140.2 (α-pyrrole), 143.1 (β-pyrrole), 146.0 (C^7), 147.0 (C^{14}), 152.8 (C^1). Anal. Calcd for $C_{79}H_{99}ClF_3N_6O_{10}Rh$: C 63.77, H 6.71, N 5.65; found: C 64.04, H 6.89, N 5.34%.

Rotaxane Rx(TBPP·S). Purple solid (Yield: 25%). ^{1}H NMR (400 MHz, $CDCl_3$): δ 1.04 (d, $J = 7.0$ Hz, 2H, C^7H), 1.14 (s, 3H, C^aH_3), 1.51 (s, 9H, *t*-Bu), 2.51 (br, 4H, $C^\gamma H_2$), 2.85 (br, 4H, $C^\gamma H_2$), 2.97 (m, 4H, $C^\beta H_2$), 3.31 (m, 4H, $C^\beta H_2$), 3.31 (overlapping, 2H, C^cH_2), 3.36 (m, 4H, $C^\alpha H_2$), 3.70 (m, 4H, $C^\alpha H_2$), 4.04 (s, 2H, C^bH_2), 5.07 (d, $J = 7.0$ Hz, 2H, C^6H), 6.19 (m, 4H, $C^{13}H$), 6.67 (m, 4H, $C^{12}H$), 6.90 (d, $J = 8.4$ Hz, 2H, C^3H), 7.00 (d, $J = 8.4$ Hz, 2H, C^2H), 7.80 (s, 4H, $C^{15}H$), 8.05 (s, 4H, $C^{17}H$), 8.14 (s, 4H, $C^{17}H$), 9.03 (s, 8H, β-pyrrole). ^{13}C NMR (100 MHz, $CDCl_3$): δ 31.6 (C^a), 32.2 (*t*-Bu), 35.0 (C–$C^a{}_3$), 35.4 (*t*-Bu), 35.6 (*t*-Bu), 49.0 (C^c), 52.2 (C^b), 68.2 (C^α), 69.9 (C^β), 70.2 (C^γ), 113.1 (C^{13}), 121.5 (C^{15}), 122.2 (C^{12}), 122.8 (C^6), 122.8 (*meso*), 125.7 (C^2), 128.6 (C^4), 129.4 (C^{17}), 129.6 (C^3), 131.5 (C^{17}), 133.0 (β-pyrrole), 141.2 (C^5), 141.6 (C^{18}), 143.0 (α-pyrrole), 146.1 (C^7), 147.0 (C^{14}), 148.8 (C^{16}), 149.7 (C^{16}), 152.7 (C^1). Anal. Calcd for $C_{119}H_{147}ClF_3N_6O_{10}Rh{\cdot}2H_2O$: calcd C 69.62, H 7.41, N 4.09; found: C 69.42, H 7.44, N 4.08%.

Results and discussion

Six kinds of porphyrin-stoppered rotaxanes were prepared by the combination of two threads [relatively longer (L) and shorter (S)] and three porphyrins (OEP, TPP and TBPP). DB24C8 was used as the macrocycle. Rx(OEP·S) represents OEP-stoppered rotaxane consisting of the macrocycle DB24C8 and thread S (Fig. 1). All of the rotaxanes excluding Rx(TBPP·S) were obtainable in high yields (70%–80%).

In the previous study,[6] we confirmed that the *pseudo*-rotaxane with relatively longer thread [*pseudo*-Rx(L): inclusion complex without porphyrin stopper] was a slow exchange system on the NMR timescale, indicating that the mixture containing the thread and macrocycle afforded two sets of peaks assignable to free and inclusion complex species in the ^{1}H NMR spectrum. From the comparison of ^{1}H NMR spectra for the rotaxane and *pseudo*-Rx(L), we confirmed the shielding effect by the terminal porphyrin, that is, all of the peaks assigned to the macrocycle and thread shifted up-field after introduction of the terminal porphyrin. We calculated the difference in the chemical shifts between *pseudo*-Rx(L) and Rx(X·Y) [$\Delta\delta = \delta_{\text{pseudo-Rx(L)}} - \delta_{\text{Rx(X·Y)}}$], which is a good probe to analyze the conformational changes in the rotaxane.

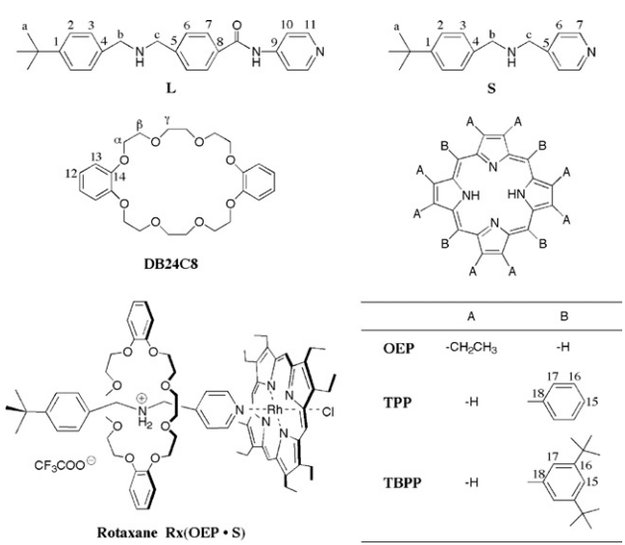

Fig. 1 Chemical structure of the components of porphyrin-stoppered rotaxanes and numbering for ^{1}H NMR assignment.

First, we focused on the protons on the macrocycle. Fig. 2 shows the $\Delta\delta$ values for each proton on the macrocycle (12, 13, α, β and γ). In the cases of the rotaxanes with relatively shorter thread [Rx(X·S)], two methylene protons on the same carbon have different chemical shifts, because the intensity of the shielding effect by the terminal porphyrin is significantly different at the near and far side methylene protons (Fig. 3).[6] Therefore, these protons were separately plotted in Fig. 2 (* and **).

In the cases of the rotaxanes with relatively longer thread [Rx(X·L)], the $\Delta\delta$ values for Rx(OEP·L) were larger than those for the other two rotaxanes [Rx(TPP·L), Rx(TBPP·L)] because four phenyl groups of TPP, which stand perpendicularly with respect to the porphyrin core,[6,10] weaken the shielding effect by the porphyrin core. The $\Delta\delta$ values for Rx(OEP·L) monotonically increase from the protons 12 to γ, because the shielding intensity by the terminal porphyrin increases from 12 to γ. The shielding intensity is the strongest at the porphyrin center, and it decreases toward the periphery.[8] As shown in Fig. 4, the protons 12, 13, α, β and γ gradually draw closer to the porphyrin center. The $\Delta\delta$ values for two rotaxanes Rx(TPP·L) and Rx(TBPP·L) were almost the same, suggesting that the conformations of the macrocycles in Rx(TPP·L) and Rx(TBPP·L) should be almost the same. In rotaxanes Rx(X·L), the affinity site of the thread and macrocycle, which is the secondary ammonium cation group,[11] is far from the terminal porphyrin. Thus, it is considered that the substituents of the porphyrins [ethyl-, phenyl- and 3,5-di(*t*-butyl)phenyl-] have no effect on the conformation of the macrocycle.

On the other hand, the results for the rotaxanes with relatively shorter thread [Rx(X·S)] were complicated. The $\Delta\delta$ values for the rotaxane Rx(OEP·S) monotonically increase from the protons 12 to γ (average $\Delta\delta$ value of near and far sides methylene protons), suggesting that the conformations of the macrocycles in Rx(OEP·L) and Rx(OEP·S) should be almost the same. Interestingly, the plots of Rx(TPP·S) and Rx(TBPP·S) were completely different from each other. In particular, the $\Delta\delta$ values for the catechol protons in Rx(TBPP·S)

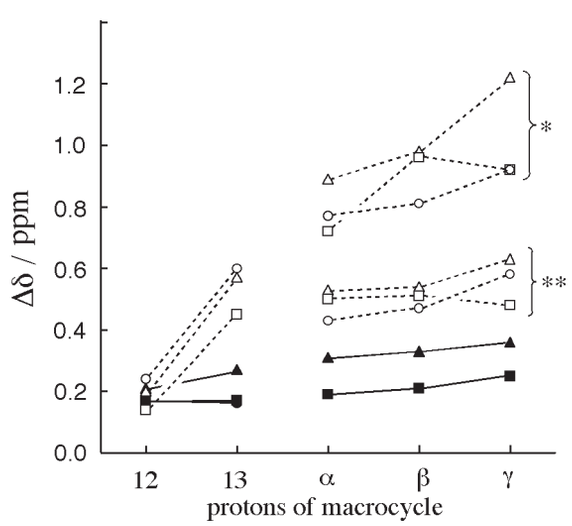

Fig. 2 Chemical shift change for each proton on the macrocycle. The $\Delta\delta$ values were calculated from the chemical shift difference between *pseudo*-rotaxane and porphyrin-stoppered rotaxane ($\Delta\delta = \delta_{\text{pseudo-Rx(L)}} - \delta_{\text{Rx(X·Y)}}$). * and ** are $\Delta\delta$ values for near and far side methylene protons with respect to the terminal porphyrin, respectively. Open triangle (△): Rx(OEP·S), open square (□): Rx(TPP·S), open circle (○): Rx(TBPP·S), closed triangle (▲): Rx(OEP·L), closed square (■): Rx(TPP·L), closed circle (●): Rx(TBPP·L). The plots of Rx(TPP·L) and Rx(TBPP·L) are overlapped.

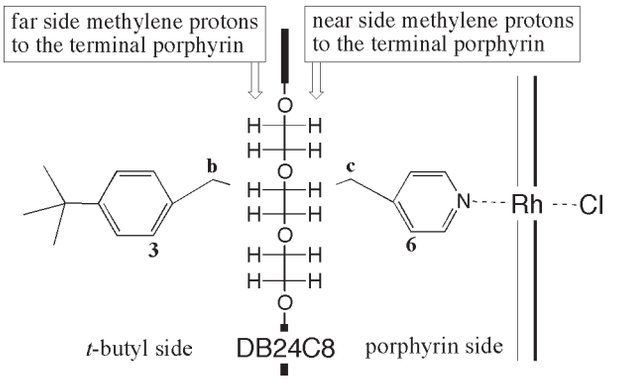

Fig. 3 Schematic illustration of the methylene protons on the macrocycle (DB24C8). In the rotaxane with relatively shorter thread, two methylene protons on the same carbon located at opposite sides are assigned to different peaks in ^{1}H NMR spectrum.

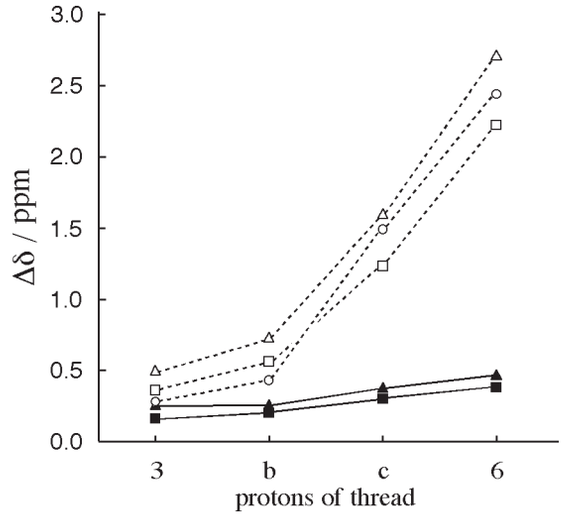

Fig. 5 Chemical shift change for each proton on the thread. The $\Delta\delta$ values were calculated from the chemical shift difference between *pseudo*-rotaxane and porphyrin-stoppered rotaxane ($\Delta\delta = \delta_{\text{pseudo-Rx(L)}} - \delta_{\text{Rx(X·Y)}}$). Open triangle (△): Rx(OEP·S), open square (□): Rx(TPP·S), open circle (○): Rx(TBPP·S), closed triangle (▲): Rx(OEP·L), closed square (■): Rx(TPP·L), closed circle (●): Rx(TBPP·L). The plots of Rx(TPP·L) and Rx(TBPP·L) are overlapped.

were larger than those in Rx(TPP·S), indicating less contribution of the deshielding effect by four phenyl groups of TBPP. The macrocycle has fast rotational conformation exchange between the conformations (A) and (B) (Fig. 4). Since the exchange rate between these two conformations is fast on the NMR timescale, the weight-averaged chemical shifts attributable to two conformations are observed in the ^{1}H NMR spectra. X-Ray crystallographic data for Rx(TPP·S) suggest that Rx(TPP·S) prefer conformation (B) due to aromatic CH–π interaction between the catechol rings and phenyl groups of TPP.[6] In the case of Rx(TBPP·S), we can easily assume that bulky *t*-butyl groups of TBPP sterically hinder conformation (B). As a consequence, the rotaxane Rx(TBPP·S) is considered to prefer conformation (A). In conformation (A), the catechol protons and the methylene protons γ are under the shielding effect of the porphyrin core, and the methylene protons α and β are under the deshielding effect of four phenyl groups [Fig. 4 (A)]. This situation is in good agreement with the results, as shown in Fig. 2. Namely, the up-field shift of the catechol protons and methylene protons γ for Rx(TBPP·S) was larger than that for Rx(TPP·S), indicating that these protons are under the shielding effect. It should be noted that the near side methylene protons to the terminal porphyrin α and γ do not follow our interpretation. In comparison with the far side methylene protons, the near side methylene protons are found to be more sensitive to the change in distance from the terminal porphyrin.[6] Thus, the effect of the conformation exchange between (A) and (B) may be easily compensated by a small distance change from the terminal porphyrin.

Next, we focused on the protons on the thread. In the case of the thread, we especially focused on the protons around the secondary ammonium cation group (3, b, c and 6) because these protons are sensitive to the conformational changes of DB24C8 due to the (de)shielding effect of the catechol rings. In the $\Delta\delta$ plot for the rotaxanes with relatively longer thread [Rx(X·L)], the result was almost the same as that discussed above (Fig. 5). The $\Delta\delta$ values for Rx(OEP·L) were larger than those for the other two rotaxanes and the $\Delta\delta$ values for Rx(TPP·L) and Rx(TBPP·L) were almost the same.

In the case of the rotaxanes with relatively shorter thread [Rx(X·S)], we found an interesting result in the comparison of Rx(TPP·S) and Rx(TBPP·S). At the *t*-butyl side (3 and b), the $\Delta\delta$ values for Rx(TPP·S) were larger than those for Rx(TBPP·S). In contrast, the $\Delta\delta$ values for the rotaxane Rx(TBPP·S) were larger than those for the rotaxane Rx(TPP·S) at the porphyrin side (c and 6). Two possible interpretations are proposed. One is that the location of the macrocycle would change toward the *t*-butyl side and the protons at this side (3 and 6) would be influenced by the stronger shielding effect of the catechol rings. The other is that the macrocycle would be in a V-shaped conformation in Rx(TBPP·S) and two catechol rings sandwich the pyridine group (Fig. 6). The latter case is supported by the up-field shift of the catechol rings in Rx(TBPP·S) (Fig. 2). It should be noted that the $\Delta\delta$ values for the catechol protons in Rx(TBPP·S) were larger than those in Rx(OEP·S), suggesting that the catechol rings in Rx(TBPP·S) are under a stronger shielding effect than those in Rx(OEP·S). It was considered that the large up-field shift of the catechol rings in Rx(TBPP·S) could be attributed to two factors, namely, contribution of conformation (A)

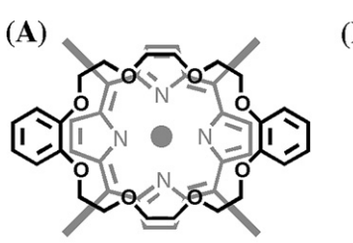

Fig. 4 Schematic illustration of two conformations arising from the rotational conformation exchange of the macrocycle in rotaxane.

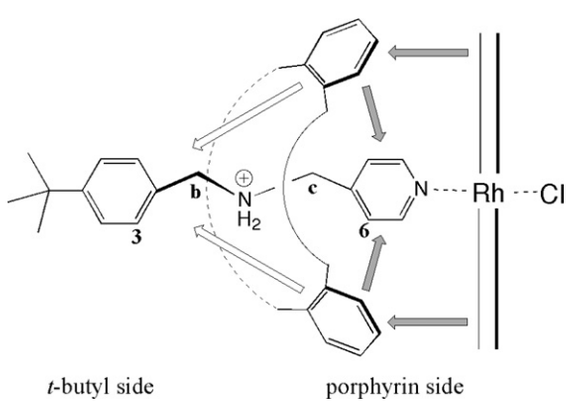

Fig. 6 Schematic illustration of the V-shaped conformation of the macrocycle in rotaxane Rx(TBPP·S). The white and gray arrows represent the deshielding and shielding effect by the aromatic planes, respectively.

(Fig. 4) and the V-shaped conformation of the macrocycle (Fig. 6). Conformation (A) enables the V-shaped conformation of the macrocycle. In conformation (B), the V-shaped conformation would be sterically hindered by the bulky *t*-butyl groups of TBPP. We considered that the conformation change of the thread would be negligible, because the thread S is very short and the interlocked macrocycle hinders a large conformational change of the thread.

Conclusion

From the analysis of the shielding effect, we were able to discuss the conformation of the macrocycle in the rotaxanes. All rotaxanes with relatively longer thread Rx(X·L) were found to be in the same conformation. However, the conformations of the macrocycle were different in the rotaxanes with relatively shorter thread Rx(X·S). In Rx(OEP·S), the conformation of the macrocycle might be almost the same as Rx(OEP·L). It is considered that the rotaxanes Rx(TBPP·S) and Rx(TPP·S) prefer conformations (A) and (B) shown in Fig. 4, respectively. Moreover, the macrocycle in Rx(TBPP·S) might be in a V-shaped conformation. The lower yield of Rx(TBPP·S) (25%) in comparison with other rotaxanes (70%–80%) suggests that the steric interaction between the macrocycle and terminal porphyrin possibly destabilizes rotaxane formation. In other words, the macrocycle mechanically interacts with TBPP in Rx(TBPP·S), which is an important aspect in designing molecular devices that can regulate the rotational motion of the macrocycle by the terminal porphyrin or transmit the rotational motion from the macrocycle to the terminal porphyrin.

Acknowledgements

This study was supported by the Industrial Technology Research Grant Program of the New Energy and Industrial Technology Development Organization (NEDO) of Japan.

References

1 R. A. Bissell, E. Córdova, A. E. Kaifer and J. F. Stoddart, *Nature*, 1994, **369**, 133; M.-V. M. Díaz, N. Spencer and J. F. Stoddart, *Angew. Chem., Int. Ed. Engl.*, 1997, **36**, 1904; P. R. Ashton, R. Ballardini, V. Balzani, A. Credi, K. R. Dress, E. Ishow, C. J. Kleverlaan, O. Kocian, J. A. Preece, N. Spencer, J. F. Stoddart, M. Venturi and S. Wenger, *Chem. Eur. J.*, 2000, **6**, 3558; A. S. Lane, D. A. Leigh and A. Murphy, *J. Am. Chem. Soc.*, 1997, **119**, 11 092; G. Bottari, F. Dehez, D. A. Leigh, P. J. Nash, E. M. Pérez, J. K. Y. Wong and F. Zerbetto, *Angew. Chem., Int. Ed.*, 2003, **42**, 5886; J. P. Collin, P. Gavina and J. P. Sauvage, *New J. Chem.*, 1997, **21**, 525; N. Armaroli, V. Balzani, J. P. Collin, P. Gavina, J. P. Sauvage and B. Ventura, *J. Am. Chem. Soc.*, 1999, **121**, 4397; H. Murakami, A. Kawabuchi, K. Kottoo, M. Kunitake and N. Nakashima, *J. Am. Chem. Soc.*, 1997, **119**, 7605.

2 Y. Chen, G. Jung, D. A. A. Ohlberg, X. Li, D. R. Stewart, J. O. Jeppesen, K. A. Nielsen, J. F. Stoddart and R. S. Williams, *Nanotechnology*, 2003, **14**, 462; A. R. Pease, J. O. Jeppesen, J. F. Stoddart, Y. Luo, C. P. Collier and J. R. Heath, *Acc. Chem Res.*, 2001, **34**, 433.

3 D. A. Leigh, J. K. Y. Wong, F. Dehez and F. Zerbetto, *Nature*, 2003, **424**, 174.

4 M. C. Jimenez, C. D. Buchecker and J. P. Sauvage, *Angew. Chem., Int. Ed.*, 2000, **39**, 3284.

5 M. Asakawa, T. Ikeda, N. Yui and T. Shimizu, *Chem. Lett.*, 2002, 174.

6 T. Ikeda, M. Asakawa, M. Goto, Y. Nagawa and T. Shimizu, *Eur. J. Org. Chem.*, 2003, 3744.

7 M. Fujita, N. Fujita, K. Ogura and K. Yamaguchi, *Nature*, 1999, **400**, 52; C. D. Buchecker, B. Colasson, M. Fujita, A. Hori, N. Geum, S. Sakamoto, K. Yamaguchi and J. P. Sauvage, *J. Am. Chem. Soc.*, 2003, **125**, 5717.

8 H. Ogoshi, J. Setsume, T. Omura and Z. Yoshida, *J. Am. Chem. Soc.*, 1975, **97**, 6461.

9 H. Tamiaki, S. Suzuki and K. Maruyama, *Bull. Chem. Soc. Jpn.*, 1993, **66**, 2633.

10 G. B. Jameson, J. P. Collman and R. Boulatov, *Acta Crystallogr., Sect. C*, 2001, **57**, 406.

11 S. J. Cantrill, A. R. Pease and J. F. Stoddart, *J. Chem. Soc., Dalton Trans.*, 2000, 3715; T. Takata and N. Kihara, *Rev. Heteroatom. Chem.*, 2000, **22**, 197.